

Optical Properties of and Spin Interaction in the Trinuclear Compound $\{[\text{Mn}(\text{Me}_6\text{-[14]ane-N}_4)]_2\text{Cu(pba)}\}(\text{CF}_3\text{SO}_3)_2 \cdot 2\text{H}_2\text{O}$

Corine Mathonière and Olivier Kahn*

Laboratoire de Chimie Inorganique, URA No. 420, Université de Paris Sud, 91405 Orsay, France

Received October 8, 1993*

The goal of this paper is to study to what extent information on the interaction between magnetic centers in a $\text{Mn}^{\text{II}}\text{Cu}^{\text{II}}\text{Mn}^{\text{II}}$ molecular compound can be deduced from the optical spectra. The compound of interest is $\{[\text{Mn}(\text{Me}_6\text{-[14]ane-N}_4)]_2\text{Cu(pba)}\}(\text{CF}_3\text{SO}_3)_2 \cdot 2\text{H}_2\text{O}$ with $\text{Me}_6\text{-[14]ane-N}_4 = (\pm)\text{-5,7,7,12,14,14-hexamethyl-1,4,8,11-tetraazacyclotetradecane}$ and $\text{pba} = 1,3\text{-propylenebis(oxamate)}$. A central $\text{Cu}(\text{II})$ ion is bridged by oxamate groups to two peripheral $\text{Mn}(\text{II})$ ions. The absorption spectra have been recorded both in pyridine solution at room temperature and in KBr pellets in the 10–290 K temperature range. These spectra, in addition to a d–d transition at 613 nm due to $\text{Cu}(\text{II})$ in square planar surroundings, exhibit narrow and rather intense $\text{Mn}(\text{II})$ spin-forbidden transitions in the 360–424-nm range. These transitions are activated by an exchange mechanism. The temperature dependence of the intensity of the $\text{Mn}(\text{II})$ ${}^6\text{A}_1, {}^6\text{A}_1 \rightarrow {}^6\text{A}_1, {}^4\text{A}_1$ excitation corresponding to the spin flip of an electron on its orbital was investigated. It has been shown that this transition is the envelope of 16 subtransitions, the relative intensities of which have been calculated using a model proposed by Tanabe and co-workers. A theoretical expression for the temperature dependence of the intensity of this transition has then been derived; this expression only depends on the J interaction parameter with $\text{Mn}(\text{II})$ and $\text{Cu}(\text{II})$ ions in their local ground states. By least-squares fitting of the experimental data, J has been found to be equal to -28.2 cm^{-1} . The energy of this transition is shifted by 68 cm^{-1} toward the high energies as the temperature is lowered. This energy shift depends on both J and the interaction parameter J^* between the $\text{Cu}(\text{II})$ ion in its ground state and the $\text{Mn}(\text{II})$ ions in the spin-flip excited state. By simulation of the spectra, J^* has been found as -45 cm^{-1} . These results have been discussed, and the consistency and the complementarity with the information deduced from magnetic properties have been emphasized.

Introduction

For several years we have been studying heterobimetallic species, in particular those with the $\text{Mn}(\text{II})$ and $\text{Cu}(\text{II})$ ions.^{1–13} Up to now, our main concern was to design in a controlled fashion molecular-based compounds exhibiting a spontaneous magnetization below a critical temperature T_c . Along this line, we reported on $\text{Mn}^{\text{II}}\text{Cu}^{\text{II}}$ ferrimagnetic chains^{1–3,5–9} and $\text{Mn}^{\text{II}}_2\text{Cu}^{\text{II}}_3$ planar networks¹² showing a three-dimensional magnetic ordering with T_c in the 4–30 K temperature range. Very recently, we described a molecular-based magnet with a fully interlocked three-dimensional structure containing a radical cation in addition to $\text{Mn}(\text{II})$ and $\text{Cu}(\text{II})$ ions as spin carriers.¹¹

In addition to their magnetic properties, these $\text{Mn}^{\text{II}}\text{Cu}^{\text{II}}$ compounds present peculiar optical properties; their absorption

spectra generally show very intense formally spin-forbidden $\text{Mn}(\text{II})$ transitions, activated by an exchange mechanism.^{7,9,10,13} The temperature dependence of the intensities and energies of these transitions may provide quantitative information on the interaction between $\text{Mn}(\text{II})$ and $\text{Cu}(\text{II})$ ions, in both the low-lying and excited molecular states. A great deal of effort has already concerned the spectroscopy of exchange-coupled systems,^{14–32} but essentially in doped systems and not in genuine bimetallic molecular species, so that the information deduced from the optical studies could not be compared to the results of magnetic measurements.

Recently, we investigated the optical and magnetic properties of a binuclear compound of formula $[\text{Mn}(\text{Me}_6\text{-[14]ane-N}_4)]_2\text{Cu(oxpn)}(\text{CF}_3\text{SO}_3)_2$, with $\text{Me}_6\text{-[14]ane-N}_4 = (\pm)\text{-5,7,7,12,14,14-hexamethyl-1,4,8,11-tetraazacyclotetradecane}$ and

* Abstract published in *Advance ACS Abstracts*, April 15, 1994.

- (1) Pei, Y.; Verdager, M.; Kahn, O.; Sletten, J.; Renard, J. P. *Inorg. Chem.* **1987**, *26*, 138.
- (2) Kahn, O. *Struct. Bonding (Berlin)* **1987**, *68*, 89.
- (3) Kahn, O.; Pei, Y.; Verdager, M.; Renard, J. P.; Sletten, J. *J. Am. Chem. Soc.* **1988**, *110*, 782.
- (4) Pei, Y.; Journaux, Y.; Kahn, O. *Inorg. Chem.* **1988**, *27*, 399.
- (5) Nakatani, K.; Carriat, J. Y.; Journaux, Y.; Kahn, O.; Lloret, F.; Renard, J. P.; Pei, Y.; Sletten, J.; Verdager, M. *J. Am. Chem. Soc.* **1989**, *111*, 5739.
- (6) Pei, Y.; Nakatani, K.; Kahn, O.; Sletten, J.; Renard, J. P. *Inorg. Chem.* **1989**, *28*, 3171.
- (7) Nakatani, K.; Kahn, O.; Mathonière, C.; Pei, Y.; Zakine, C. *New J. Chem.* **1990**, *14*, 861.
- (8) Nakatani, K.; Sletten, J.; Halut-Desporte, S.; Jeannin, S.; Jeannin, Y.; Kahn, O. *Inorg. Chem.* **1991**, *30*, 164.
- (9) Pei, Y.; Kahn, O.; Nakatani, K.; Codjovi, E.; Mathonière, C.; Sletten, J. *J. Am. Chem. Soc.* **1991**, *113*, 6558.
- (10) Nakatani, K.; Bergerat, P.; Codjovi, E.; Mathonière, C.; Pei, Y.; Kahn, O. *Inorg. Chem.* **1991**, *30*, 3977.
- (11) Stumpf, H. O.; Ouahab, L.; Pei, Y.; Grandjean, D.; Kahn, O. *Science* **1993**, *261*, 447.
- (12) Stumpf, H. O.; Pei, Y.; Kahn, O.; Renard, J. P. *J. Am. Chem. Soc.* **1993**, *115*, 6738.
- (13) Mathonière, C.; Kahn, O.; Daran, J. C.; Hilbig, H.; Kölher, F. H. *Inorg. Chem.* **1993**, *32*, 4057.

- (14) Güdel, H. U. In *Magneto-Structural Correlations in Exchange Coupled Systems*; Willett, R. D., Gatteschi, D., Kahn, O., Eds.; Reidel: Dordrecht, The Netherlands, 1985; p 297.
- (15) McCarthy, P. J.; Güdel, H. U. *Coord. Chem. Rev.* **1988**, *88*, 69.
- (16) Ferguson, J.; Guggenheim, H. J.; Tanabe, Y. *J. Phys. Soc. Jpn.* **1966**, *21*, 692.
- (17) Ferguson, J.; Guggenheim, H. J.; Tanabe, Y. *J. Chem. Phys.* **1966**, *45*, 1134.
- (18) Ferguson, J.; Guggenheim, H. J.; Tanabe, Y. *Phys. Rev.* **1967**, *161*, 207.
- (19) Ferguson, J.; Güdel, H. U.; Krausz, E. R.; Guggenheim, H. J. *Mol. Phys.* **1974**, *28*, 893.
- (20) Ferguson, J.; Güdel, H. U.; Krausz, E. R. *Mol. Phys.* **1975**, *30*, 1139.
- (21) Ferguson, J.; Guggenheim, H. J. *Phys. Rev. B* **1970**, *1*, 4223.
- (22) Ferguson, J.; Guggenheim, H. J.; Krausz, E. R. *J. Phys. C: Solid State Phys.* **1971**, *4*, 1866.
- (23) Ferguson, J.; Fielding, P. E. *Aust. J. Chem.* **1972**, *25*, 1371.
- (24) Ferré, J.; Regis, M. *Solid State Commun.* **1978**, *26*, 225.
- (25) Ferguson, J.; Masui, H. *J. Lumin.* **1979**, *18–19*, 224.
- (26) Wiltshire, M. C. K. *J. Phys. C: Solid State Phys.* **1982**, *15*, 4177.
- (27) Wood, T. E.; Cox, P. A.; Day, P.; Walker, X. *J. Phys. C: Solid State Phys.* **1982**, *15*, L787.
- (28) McCarthy, P. J.; Güdel, H. U. *Inorg. Chem.* **1984**, *23*, 880.
- (29) Jacobsen, S. M.; Güdel, H. U.; Smith, W. E. *Inorg. Chem.* **1987**, *26*, 2001.
- (30) Herren, M.; Jacobsen, S. M.; Güdel, H. U.; Briat, B. *J. Chem. Phys.* **1989**, *2*, 663.
- (31) Herren, M.; Jacobsen, S. M.; Güdel, H. U. *Inorg. Chem.* **1989**, *28*, 504.
- (32) Herren, M.; Güdel, H. U. *J. Lumin.* **1992**, *54*, 209.

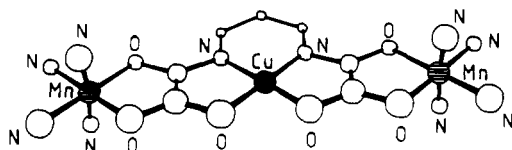


Figure 1. Schematic representation of the trinuclear cation $\{[\text{Mn}(\text{Me}_6\text{-[14]ane-N}_4)_2\text{Cu}(\text{pba})]\}^{2+}$. For the sake of simplicity, only the nitrogen atoms of the peripheral ligands $\text{Me}_6\text{-[14]ane-N}_4$ have been represented.

oxpn = *N,N'*-bis(3-aminopropyl)oxamide.¹³ The interaction between the local ground states characterized by $S_{\text{Mn}} = 5/2$ and $S_{\text{Cu}} = 1/2$ gives rise to $S = 2$ and $S = 3$ low-lying pair states. The interaction between the Mn(II) excited local state characterized by $S_{\text{Mn}}^* = 3/2$ and the Cu(II) ground state gives rise to $S^* = 1$ and $S^* = 2$ excited pair states. The $S_{\text{Mn}} = 5/2 \rightarrow S_{\text{Mn}}^* = 3/2$ spin-forbidden transition for the isolated Mn(II) ion corresponds to the $S = 2 \rightarrow S^* = 2$ spin-allowed transition for the $\text{Mn}^{\text{II}}\text{Cu}^{\text{II}}$ pair. The intensity of this transition varies as the thermal population of the $S = 2$ pair state, so that the interaction parameter J between the local ground states may be easily deduced from the temperature dependence of this intensity. In the case of $[\text{Mn}(\text{Me}_6\text{-[14]ane-N}_4)\text{Cu}(\text{oxpn})](\text{CF}_3\text{SO}_3)_2$, the J value deduced from the optical data is identical within the experimental uncertainties to that deduced from magnetic susceptibility measurements, namely $J = -31 \text{ cm}^{-1}$. This agreement encouraged us to investigate the optical properties of $\text{Mn}^{\text{II}}\text{Cu}^{\text{II}}$ compounds of higher nuclearity. In this paper, we report the results obtained with the trinuclear species of formula $\{[\text{Mn}(\text{Me}_6\text{-[14]ane-N}_4)_2\text{Cu}(\text{pba})]\}(\text{CF}_3\text{SO}_3)_2 \cdot 2\text{H}_2\text{O}$, hereafter abbreviated as MnCuMn where pba stands for 1,3-propylenebis(oxamato). The synthesis and the magnetic and EPR properties of this $\text{Mn}^{\text{II}}\text{Cu}^{\text{II}}\text{Mn}^{\text{II}}$ trinuclear species have been described elsewhere.⁴ We will show that the study of the optical properties may lead to the interaction parameters between Mn^{II} and Cu^{II} ions not only when these ions are in their local ground states but also when one of the Mn(II) ions is in its local spin-flip excited state. These pieces of information, however, require rather complicated calculations.

The molecular structure of MnCuMn is not known accurately. By analogy with other $\text{Mn}^{\text{II}}\text{Cu}^{\text{II}}$ compounds whose structures were determined by X-ray diffraction,^{1,3} and with a NiCuNi trinuclear compound with the same bridge,³³ this trinuclear compound may be represented as shown in Figure 1.⁴ The molecular symmetry may be idealized in D_{2h} ; a square planar Cu(II) ion at the center interacts with two octahedral Mn(II) ions at the periphery.

Experimental Section

$\{[\text{Mn}(\text{Me}_6\text{-[14]ane-N}_4)_2\text{Cu}(\text{pba})]\}(\text{CF}_3\text{SO}_3)_2 \cdot 2\text{H}_2\text{O}$ was synthesized as previously described in the form of a polycrystalline powder.⁴ The absorption spectra were recorded with a Varian 2300 spectrometer equipped with a closed-circuit cryostat provided by Air Products. The spectra were studied both in pyridine solution and in KBr pellets fixed on a copper plate with silver paint. The lowest temperature which can be reached is 10 K. The band intensities in the solid state were calculated from the area delimited by the absorption bands and a baseline common to all spectra.

Description of the Spectra

The absorption spectrum of MnCuMn in pyridine solution at room temperature is shown in Figure 2. This spectrum displays a broad band at 613 nm ($16\,313 \text{ cm}^{-1}$; $\epsilon = 232 \text{ L mol}^{-1} \text{ cm}^{-1}$), a rather intense and narrow band at 424 nm ($23\,585 \text{ cm}^{-1}$; $\epsilon = 550 \text{ L mol}^{-1} \text{ cm}^{-1}$), two shoulders at 397 nm ($25\,189 \text{ cm}^{-1}$) and 385 nm ($25\,974 \text{ cm}^{-1}$), and the most intense band at 363 nm

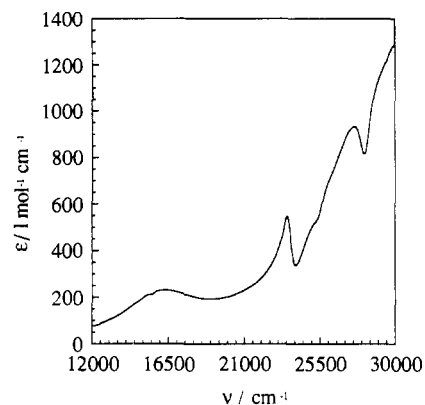
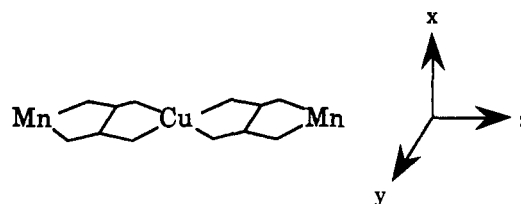


Figure 2. Absorption spectrum of $\{[\text{Mn}(\text{Me}_6\text{-[14]ane-N}_4)_2\text{Cu}(\text{pba})]\}(\text{CF}_3\text{SO}_3)_2 \cdot 2\text{H}_2\text{O}$ in pyridine solution.

($27\,548 \text{ cm}^{-1}$; $\epsilon = 933 \text{ L mol}^{-1} \text{ cm}^{-1}$). The band at 613 nm is characteristic of a Cu(II) in square planar environment. It corresponds to the ${}^2\text{B}_{3g} \rightarrow {}^2\text{A}_{1g}$ local transition, assuming a D_{2h} symmetry and using the following reference axes:



The bands in the high-energy range of the spectrum correspond to formally spin-forbidden transitions of Mn(II). The narrow band at 424 nm corresponds to the ${}^6\text{A}_1 \rightarrow {}^4\text{A}_1(\text{G}) + {}^4\text{E}(\text{G})$ transition of Mn(II) in cubic symmetry; this transition is not influenced at the first order by the ligand field, as there is no electron jump between t_{2g} and e_g metal orbitals. By analogy with the spectra of other octahedral Mn(II) species,³⁴ the bands at 385 and 363 nm can be assigned to ${}^6\text{A}_1 \rightarrow {}^4\text{T}_2(\text{D})$ and ${}^6\text{A}_1 \rightarrow {}^4\text{E}(\text{D})$ transitions, respectively. The origin of the shoulder at 397 nm is not clear.

The spectrum of MnCuMn in KBr pellets with a concentration of 3% at room temperature is similar to the spectrum in pyridine solution. When the temperature is lowered, the band associated with the Cu(II) ion is essentially unchanged. In contrast, the intensity of the bands associated with the Mn(II) ion increases by roughly a factor 2 between 300 and 10 K. Furthermore, owing to the narrowness of the ${}^6\text{A}_1 \rightarrow {}^4\text{A}_1(\text{G}) + {}^4\text{E}(\text{G})$ transition, it is possible to follow the temperature dependence of its energy. A careful analysis of the first derivatives of this band shows that the energy is shifted from $23\,577 \text{ cm}^{-1}$ at 290 K up to $23\,645 \text{ cm}^{-1}$ at 10 K. The shift is then 68 cm^{-1} .

Quantitative Interpretation

In this section, which represents the heart of the paper, we will focus on the ${}^6\text{A}_1 \rightarrow {}^4\text{A}_1(\text{G}) + {}^4\text{E}(\text{G})$ transition corresponding to the spin flip of an electron of Mn(II) on its orbital, and we will analyze the temperature dependence of its intensity (see Figure 3) and then of its energy. Works on Mn(II) pairs have shown that the intensity of the ${}^4\text{E}$ excitation is much weaker than that of the ${}^4\text{A}_1$ excitation,¹⁷⁻¹⁹ and in the following we will assume that the intensity of the band at 424 nm arises from this ${}^4\text{A}_1$ excitation. The validity of this assumption will be discussed in the following section. For this study, we will use the D_{2h} idealized symmetry.

(33) Ribas, J.; Diaz, C.; Costa, R.; Journaux, Y.; Mathonière, C.; Kahn, O.; Gleizes, A. *Inorg. Chem.* **1990**, *29*, 2042.

(34) Lever, A. B. P. *Inorganic Electronic Spectroscopy*, 2nd ed.; Elsevier: Amsterdam, 1984.

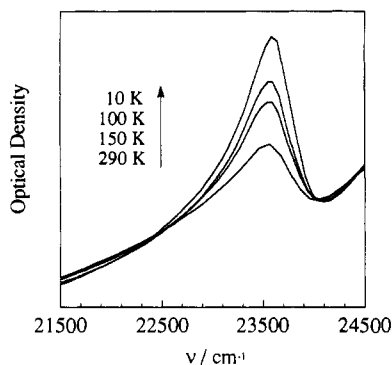


Figure 3. Absorption bands at 424 nm for $\{[\text{Mn}(\text{Me}_6\text{-[14]ane-N}_4)]_2\text{Cu}(\text{pba})\}(\text{CF}_3\text{SO}_3)_2 \cdot 2\text{H}_2\text{O}$ in KBr pellets at various temperatures.

The spin Hamiltonian describing the interaction between the local ground states can be written as

$$\mathbf{H} = -\mathbf{J}\mathbf{S}_{\text{Cu}} \cdot \mathbf{S}_{\text{Mn}} \quad (1)$$

$$\mathbf{S}_{\text{Mn}} = \mathbf{S}_{\text{Mn1}} + \mathbf{S}_{\text{Mn2}} \quad (2)$$

where \mathbf{S}_{Cu} , \mathbf{S}_{Mn1} , and \mathbf{S}_{Mn2} are the local spins. In (1) local anisotropy and anisotropic interactions have been neglected as well as the interaction between the peripheral Mn(II) ions separated by ca. 11 Å. This Hamiltonian leads to 11 low-lying states $|S, S_{\text{Mn}}\rangle$ whose relative energies are given by

$$E(S, S_{\text{Mn}}) = -J[S(S+1) - S_{\text{Mn}}(S_{\text{Mn}}+1)]/2 \quad (3)$$

S and S_{Mn} being the quantum numbers associated with the spin operators $\mathbf{S} = \mathbf{S}_{\text{Cu}} + \mathbf{S}_{\text{Mn}}$ and \mathbf{S}_{Mn} , respectively. It is interesting at this stage to look for the symmetry labels of these states. The site symmetry of each Mn(II) ion is C_{2v} (assuming always a D_{2h} molecular symmetry), and the local ground state is 6A_1 . The coupling between the Mn(II) ions gives rise to ${}^1A_g + {}^3B_{1u} + {}^5A_g + {}^7B_{1u} + {}^9A_g + {}^{11}B_{1u}$ pair states in D_{2h} . The interaction with the ${}^2B_{3g}$ local ground state of Cu(II) leads to the symmetry labels given in Figure 4.

Let us consider now the excited states resulting from the spin flip on one Mn(II) ion. \mathbf{S}^*_{Mn} is the spin operator associated with the two Mn(II) ions, the total spin being now $\mathbf{S} = \mathbf{S}_{\text{Cu}} + \mathbf{S}^*_{\text{Mn}}$. The quantum number \mathbf{S}^*_{Mn} varies by an integer value from 1 to 4. The excited local state of the Mn(II) ion is 4A_1 in C_{2v} . The coupling of the two Mn(II) ions leads to ${}^3A_g + {}^3B_{1u} + {}^5A_g + {}^5B_{1u} + {}^7A_g + {}^7B_{1u} + {}^9A_g + {}^9B_{1u}$ pair states. Coupling further the Mn(II) pair with the central Cu(II) ion results in the symmetry labels of the excited states indicated in Figure 4. In contrast with what happens for the low-lying states, to each $|S, S^*_{\text{Mn}}\rangle$ label correspond two states, one symmetric (g) and the other one antisymmetric (u) with respect to the inversion. This is due to the fact that the spin flip may occur on either Mn(II) ion. In the following, we will assume that, owing to the separation between the Mn(II) ions, the splitting between the $|S, S^*_{\text{Mn},g}\rangle$ and $|S, S^*_{\text{Mn},u}\rangle$ states is negligible. This approximation is consistent with the fact that the interaction between the peripheral Mn(II) ions has been neglected.

Straightforward group symmetry considerations and the Laporte rule indicate that the active subtransitions are of the type ${}^{2S+1}B_{3g} \rightarrow {}^{2S+1}B_{2u}$ and ${}^{2S+1}B_{2u} \rightarrow {}^{2S+1}B_{3g}$. These transitions are 16 in number; they are all polarized along the z axis joining the metal atoms.

The problem with which we are faced now is to determine the relative intensities of the 16 subtransitions. For that, we assume that these subtransitions are activated by the mechanism proposed by Tanabe and co-workers.¹⁶ This mechanism is expected to

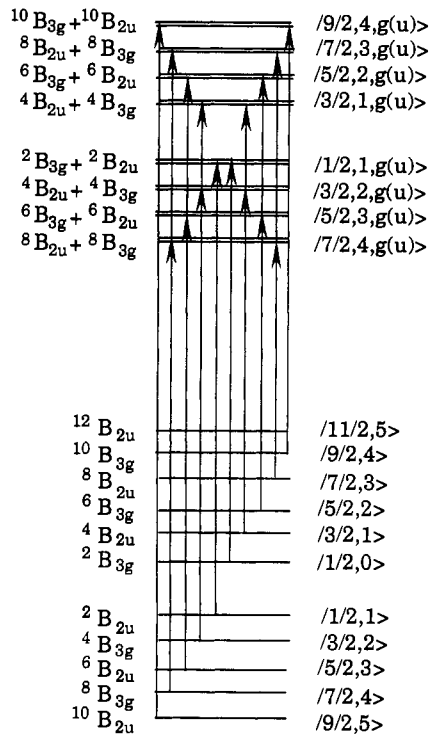


Figure 4. Relative energies and symmetry labels for the low-lying and excited states for $\{[\text{Mn}(\text{Me}_6\text{-[14]ane-N}_4)]_2\text{Cu}(\text{pba})\}(\text{CF}_3\text{SO}_3)_2 \cdot 2\text{H}_2\text{O}$ (see text).

describe properly the experimental data when the transitions occur between states arising from the same orbital configuration, i.e. when they are associated with the spin flip of an electron on its orbital, which is the case for the band we focus on.

According to Tanabe and co-workers,¹⁶ the Hamiltonian describing the interaction between MnCuMn and the electric field of the light, \mathbf{E} , may be written as

$$\mathbf{H}_E = \sum_{i=1}^5 [(\Pi_{\text{Mn1Cu}} \cdot \mathbf{E})(s_{\text{Mn1}} \cdot \mathbf{S}_{\text{Cu}})] \quad (4)$$

$$\Pi_{\text{Mn1Cu}} = \Pi_{\text{Mn1Cu}} + \Pi_{\text{Mn2Cu}} \quad (5)$$

where $s_{\text{Mn}i}$ is a mono-electronic spin operator referring to the i th d-type orbital of a Mn(II) ion. The components of the Π_{Mn1Cu} vector are of the form

$$\Pi_{\text{Mn1Cu}}^t = (\partial J_i / \partial E^t) \quad E^t \rightarrow 0 \quad t = x, y, z \quad (6)$$

where J_i represents the interaction parameter between the i th orbital of Mn(II) and the unique magnetic orbital of Cu(II). The components of Π_{Mn2Cu} are given by similar expressions. In MnCuMn, each fragment MnCu has a C_{2v} symmetry. In order for \mathbf{H}_E in (4) to be totally symmetric, Π_{Mn1Cu} and \mathbf{E} must transform as the same irreducible representations of C_{2v} . \mathbf{E} has the x , y , z symmetry, and the 2-fold rotation transforms x into $-x$ and y into $-y$. It follows that $\Pi_{\text{Mn1Cu}}^t = 0$ for $t = x$ and y . The exchange mechanism provides intensity only to the subtransitions polarized along the z axis. Moreover, taking into account the centrosymmetry of MnCuMn results in $\Pi_{\text{Mn1Cu}}^z = -\Pi_{\text{Mn2Cu}}^z$ for any i provided that the phases were chosen in such a way that the inversion transforms the i th orbital of Mn1 into the i th orbital of Mn2.

The transition moment vector, \mathbf{P} , is defined as

$$\mathbf{P} = \sum_{i=1}^5 \Pi_{\text{Mn1Cu}} (s_{\text{Mn1}} \cdot \mathbf{S}_{\text{Cu}}) \quad (7)$$

Table 1. Relative Intensities $I(S, S_{Mn}, S^*_{Mn})$ and $I(S, S_{Mn})$ of the Subtransitions^a

Transition	$I(S, S_{Mn}, S^*_{Mn})$	$I(S, S_{Mn})$
$^9/2, 5 \rightarrow ^9/2, 4, g$	1	1
$^7/2, 4 \rightarrow ^7/2, 3, u$	0.767	
$^7/2, 4 \rightarrow ^7/2, 4, u$	0.142	0.909
$^5/2, 3 \rightarrow ^5/2, 2, g$	0.545	
$^5/2, 3 \rightarrow ^5/2, 3, g$	0.273	0.819
$^3/2, 2 \rightarrow ^3/2, 1, u$	0.318	
$^3/2, 2 \rightarrow ^3/2, 2, u$	0.409	0.727
$^1/2, 1 \rightarrow ^1/2, 1, g$	0.636	0.636
$^1/2, 0 \rightarrow ^1/2, 1, u$	0.455	0.455
$^3/2, 1 \rightarrow ^3/2, 1, g$	0.159	
$^3/2, 1 \rightarrow ^3/2, 2, g$	0.205	0.364
$^5/2, 2 \rightarrow ^5/2, 2, u$	0.182	
$^5/2, 2 \rightarrow ^5/2, 3, u$	0.091	0.273
$^7/2, 3 \rightarrow ^7/2, 3, g$	0.153	
$^7/2, 3 \rightarrow ^7/2, 4, g$	0.028	0.181
$^9/2, 4 \rightarrow ^9/2, 4, u$	0.091	0.091

^a See text.

The matrix elements

$$P(S, S_{Mn}, S^*_{Mn}) = \langle S, S_{Mn} | P | S, S^*_{Mn}, g(u) \rangle \quad (8)$$

associated with the $|S, S_{Mn}\rangle \rightarrow |S, S^*_{Mn}, g(u)\rangle$ parity-allowed subtransition are calculated using the irreducible tensor technique (see Appendix) as

$$P(S, S_{Mn}, S^*_{Mn}) =$$

$$C \sqrt{(2S_{Mn} + 1)(2S^*_{Mn} + 1)} \begin{Bmatrix} S^*_{Mn} & 1/2 & S \\ 1/2 & S_{Mn} & 1 \end{Bmatrix} \begin{Bmatrix} S_{Mn} & 1 & S^*_{Mn} \\ 3/2 & 5/2 & 5/2 \end{Bmatrix} \quad (9)$$

where C is a vectorial constant, and the expressions between brackets are 6- j symbols. Relationship 9 leads to the spin selection rules $\Delta S = 0$, $\Delta M_S = 0$, $\Delta S_{Mn} = 0$ and ± 1 . Let us define by $I(S, S_{Mn}, S^*_{Mn})$ the intensity of the $|S, S_{Mn}\rangle \rightarrow |S, S^*_{Mn}, g(u)\rangle$ subtransition relative to the intensity of $^9/2, 5 \rightarrow ^9/2, 4, g > (^{10}B_{2u} \rightarrow ^{10}B_{3g})$

$$I(S, S_{Mn}, S^*_{Mn}) = P^2(S, S_{Mn}, S^*_{Mn}) / P^2(^9/2, 5, 4) \quad (10)$$

The $I(S, S_{Mn}, S^*_{Mn})$ relative intensities are tabulated in Table 1 together with the sum of the relative intensities of the subtransitions arising from a same low-lying level, $I(S, S_{Mn})$. The temperature dependence of the intensity of the band is then expressed as

$$I = B(^9/2, 5, T) + \sum_{S_{Mn}=0}^4 \sum_{S=|S_{Mn}-1/2|}^{S_{Mn}+1/2} I(S, S_{Mn}) B(S, S_{Mn}, T) \quad (11)$$

where $B(S, S_{Mn}, T)$ is the Boltzmann population coefficient defined as

$$B(S, S_{Mn}, T) = \frac{(2S + 1) \exp[-E(S, S_{Mn})/kT]}{\sum_{S_{Mn}=0}^5 \sum_{S=|S_{Mn}-1/2|}^{S_{Mn}+1/2} (2S + 1) \exp[-E(S, S_{Mn})/kT]} \quad (12)$$

Least-squares fitting of the experimental data leads to $J = -28.2 \text{ cm}^{-1}$. Experimental and calculated intensities are compared in Figure 5. One can see that the experiment-theory agreement is not perfect. The intensity of the transition is a bit more temperature dependent than predicted by the model.

Let us come back to the energy shift of the band mentioned in the previous section. To interpret quantitatively this shift, it

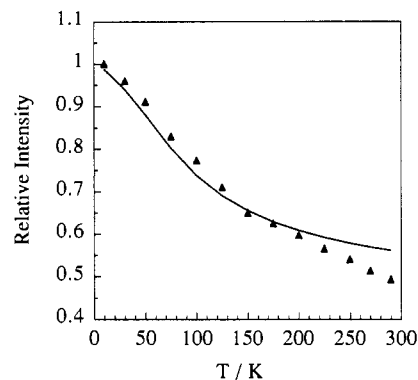


Figure 5. Temperature dependence of the absorption band at 423 nm for $\{[Mn(Me_6-14\text{ane-N}_4)]_2Cu(pba)\}(CF_3SO_3)_2 \cdot 2H_2O$: (▲) experimental data; (—) calculated curve.

is necessary to determine the energies $E(S, S^*_{Mn})$ of the spin-flip states. The general expression for the spin Hamiltonian is

$$H^* = - \sum_{i=1}^5 J_i S_{Cu} \cdot (s_{Mn/i1} + s_{Mn/i2}) \quad (13)$$

where the mono-electronic spin operator $s_{Mn/i1}$ refers to one of the Mn(II) ions and $s_{Mn/i2}$ refers to the other. Using again the irreducible tensor technique, it is found that the $E(S, S^*_{Mn})$ energies may be deduced from effective spin Hamiltonians of the form

$$H^*(S^*_{Mn}) = -J^*(S^*_{Mn}) S_{Cu} \cdot S^*_{Mn} \quad (14)$$

the $J^*(S^*_{Mn})$ interaction parameters being given by

$$\begin{aligned} J^*(1) &= 0.167J_t + 0.250J_e \\ J^*(2) &= 0.203J_t + 0.194J_e \\ J^*(3) &= 0.213J_t + 0.180J_e \\ J^*(4) &= 0.216J_t + 0.174J_e \end{aligned} \quad (15)$$

with

$$\begin{aligned} J_t &= J_1 + J_2 + J_3 \\ J_e &= J_4 + J_5 \end{aligned} \quad (16)$$

The indices 1-3 refer to orbitals arising from the t_{2g} set, and 4 and 5 to orbitals arising from the e_g set. One can see that the $J^*(S^*_{Mn})$ interaction parameters are not strictly equal but are rather close to each other. It is then possible to define an average parameter J^* as

$$J^* = [9J^*(4) + 7J^*(3) + 5J^*(2) + 3J^*(1)]/24 = 0.206J_t + 0.189J_e \quad (17)$$

We can note here that the J interaction parameter between Cu(II) and Mn(II) ions in their local ground states is given by

$$J = (J_t + J_e)/5 \quad (18)$$

At very low temperature, only the $^{10}B_{2u}$ ground state is thermally populated and the intensity entirely arises from the $^{10}B_{2u} \rightarrow ^{10}B_{3g}$ subtransition. Figure 4, in which it was assumed that J^* is negative, shows that this subtransition is the highest in energy. When the temperature increases, more and more subtransitions of lower energy become active. Since the observed band is the envelope of the 16 subtransitions, its maximum moves toward the

low energies as T increases. This energy shift allows us to estimate the J^* value. Indeed, while the temperature dependence of the intensity of the transition only depends on J , the energy of this transition depends on both J and J^* as well as on the bandwidths of the subtransitions. Assuming that the bands associated with the subtransitions are Gaussians with identical bandwidths (500 cm⁻¹) and using the J value determined above ($J = -28.2$ cm⁻¹), it is possible to reproduce the observed energy shift with $J^* = -45$ cm⁻¹.

Discussion

The interaction parameter deduced from the intensity of the Mn(II) spin-flip transition is found equal to $J = -28.2$ cm⁻¹. Two points need to be discussed: (i) this value is significantly different from that deduced from the magnetic susceptibility data, namely -36.6 cm⁻¹; (ii) the experiment-theory agreement is not perfect, in particular above 200 K.

Concerning the first point, we can note that the J value calculated from the magnetic susceptibility data is essentially governed by the characteristic minimum of the product $\chi_M T$ of the molar magnetic susceptibility and the temperature.⁴ This maximum, observed around 170 K, is very weakly pronounced. Actually, $\chi_M T$ is weakly sensitive to temperature down to ca. 80 K; as a matter of fact, $\chi_M T$ is equal to 8.83 cm³ K mol⁻¹ at 290 K, smoothly decreases as the temperature is lowered, and reaches 8.64 cm³ K mol⁻¹ at 170 K. When the temperature is lowered further, $\chi_M T$ increases, again in a smooth fashion, and reaches 8.90 cm³ K mol⁻¹ at 80 K. We are typically in a situation where the uncertainty in the J value determined from magnetic susceptibility measurements is expected to be large. In other respects, the interaction parameter between Mn(II) and Cu(II) ions through an oxamato bridge has been determined in several ferrimagnetic chains^{1,3,12} and always found to range between -24 and -32 cm⁻¹. Moreover, for the dinuclear compound [Mn(Me₆-[14]ane-N₄)Cu(oxpn)](CF₃SO₃)₂, the $\chi_M T$ versus T plot is much more contrasted than that for MnCuMn, and J can be determined accurately from the magnetic susceptibility data;¹³ it was found as -31 cm⁻¹. It is well established that, everything else being unchanged, the oxamido bridge is a bit more efficient than the oxamato bridge in transmitting an antiferromagnetic interaction between magnetic centers.³⁵ This is due to the fact that the higher electronegativity of nitrogen as compared to oxygen favors the spin delocalization. To sum up, we can say that, in the case of MnCuMn, the J value deduced from optical data seems to be more reliable than that deduced from magnetic data.

Let us consider now the difference between observed and calculated temperature dependences of the intensity. Let us mention first that this difference does not seem to be due to experimental factors. We investigated several samples and obtained much the same $I = f(T)$ curves. We then explored the various hypotheses contained in the theoretical treatment: (i) The intensity of the band at 424 nm was assumed to arise from the Mn(II) ⁴A₁ excitation. In fact, the ⁴A₁(G) state is accidentally degenerate with the ⁴E(G) state in a perfect O_h symmetry, and the asymmetry on the low-energy side of the band might be due to the low symmetry of the Mn(II) ions. Let us examine this possibility in more detail. In the C_{2v} site symmetry, ⁴E gives rise to ⁴A₁ + ⁴B₂. The local B₂ symmetry gives rise to B_{3g} + B_{2u} symmetries for the two Mn(II) ions and to A_g + B_{1u} symmetries for the MnCuMn trinuclear unit (referring to the D_{2h} molecular symmetry). All the subtransitions toward A_g and B_{1u} states would be polarized along the y axis, and we have seen that the exchange mechanism does not provide any intensity for such subtransitions. Therefore, the ⁴B₂ state arising from ⁴E(G) does not contribute to the intensity. On the other hand, the ⁴A₁ state arising from ⁴E(G) might contribute. However, if it were so, this ⁴A₁ state

would behave exactly as the other ⁴A₁ state as far as the temperature dependence is concerned. In this respect, it is worth mentioning that the asymmetry of the band does not vary versus the temperature. To sum up this point, we can say that taking into account the ⁴E(G) state does not improve the model as long as we retain the D_{2h} molecular symmetry. (ii) The interaction between Mn(II) ions is neglected. Taking into account this interaction would lead to the introduction of $\Pi_{Mn1/Mn2}$ components involving the i th orbital of Mn1 and the j th of Mn2 in the transition moments. Owing to the D_{2h} molecular symmetry, these components are all zero. (iii) The bilinear term $-J S_{Cu} \cdot S_{Mn}$, it was assumed that the energies of the low-lying states were described properly. The introduction of a biquadratic term, $j(S_{Cu} \cdot S_{Mn})^2$, does not improve the fitting; it leads to $J = -28.6$ cm⁻¹ and $j = 0.84$ cm⁻¹. (iv) The molecular symmetry was idealized in D_{2h} whereas the actual symmetry is obviously lower. Only in the D_{2h} symmetry are all the subtransitions polarized along the z axis. In a lower symmetry taking into account the distortion around the Cu(II) ion with respect to a perfect square plane, the intensities of the subtransitions do not depend anymore of the same linear combination of the $\Pi_{Mn1/Cu}$ and $\Pi_{Mn2/Cu}$ components, so that the calculation of the relative intensities cannot be performed anymore. *Only in this idealized D_{2h} symmetry can J be deduced from the optical data.* (v) Finally, the Tanabe model was assumed to be entirely valid. There is no doubt that Tanabe and co-workers contributed pioneering work to the field of the spectroscopy of coupled systems. However, to a large extent, the physical bases of their model are intuitive, and in some cases the validity of this model might be limited. A good illustration of this is provided by the study carried out by McCarthy and Güdel concerning Mn(II) pairs in both CsMgBr₃ and CsMgCl₃.²⁸ These authors resolved three of the four ⁶A₁⁶A₁ → ⁶A₁⁴A₁ transitions. The Tanabe model predicts the ratio 7/30/63 for the intensities of the spin-triplet, quintet, and septet pair states. The experimentally observed ratios are 7/15/35 for the bromide and 7/20/61 for the chloride. McCarthy and Güdel's conclusion regarding these discrepancies was "they can be due to some intensity contributions from a single-ion mechanism and to the approximations inherent in the theory". This conclusion could be retained in our case.

An important finding of our work is an estimation of the interaction between the Cu(II) ion in its ground state and the Mn(II) ions in the ⁶A₁⁴A₁ excited state. In fact, there are four different parameters $J^*(S^*_{Mn})$ describing this interaction. It seemed to us that it would be meaningless to deduce reliable values of these parameters from the only energy shift of the spin-flip transition, and we preferred to determine an average value, $J^* = -45$ cm⁻¹. The interaction in the excited state is antiferromagnetic, as in the ground state, and is of the same order of magnitude. This is probably due to the fact that the main contribution to both J and J^* is the strongly antiferromagnetic term J_{yz} involving two magnetic orbitals located in the same plane and pointing to each other.³⁵

Conclusion

This paper is the second one from our group dealing with the optical properties of Mn^{II}Cu^{II} compounds. The former paper dealt with a dinuclear species. In this simple case the intensity of the $S_{Mn} = 5/2 \rightarrow S^*_{Mn} = 3/2$ transition only depends on the population of the spin-quintet ground pair state and therefore is directly related to the $3J$ energy gap between quintet and septet low-lying states. The interaction parameter may be determined irrespective of the activation mechanism for the spin-forbidden transition.

This paper deals with a Mn^{II}Cu^{II}Mn^{II} species. The intensity of the Mn(II) ⁶A₁⁶A₁ → ⁶A₁⁴A₁ excitation now depends on the thermal populations of 10 out of a total of 11 low-lying states as well as on the relative intensities of the subtransitions arising

(35) Kahn, O. *Angew. Chem., Int. Ed. Engl.* 1985, 24, 834.

from these states. To calculate these relative intensities, it is necessary to use a model. To the best of our knowledge, the model proposed by Tanabe and co-workers is the only one available so far. In the frame of this model, the calculation can be performed only if the symmetry is idealized in D_{2h} . The intrinsic limitations of the model along with the necessary idealization of the symmetry result in some discrepancy between observed and calculated $I = f(T)$ plots. Nevertheless, the interaction parameter value to which this approach leads is quite reasonable. Actually, its value seems to be more reliable than that determined from the magnetic properties. Furthermore, the study of the optical spectrum provides some information on the interaction in the excited state which evidently could not be obtained from the magnetic properties.

In the future, we intend to investigate the optical properties of other $Mn^{II}Cu^{II}$ systems and to explore further both the consistency and the complementarity between optical and magnetic techniques.

Appendix

The matrix elements

$$P = \sum_{i=1}^5 \Pi_{MnCu} \langle S_i S_{Mn} | S_{Mn} S_{Cu} | S_i S_{Mn}^* \rangle g(u)$$

are calculated using the irreducible tensor technique³⁶ and found as

$$P = \sum_{i=1}^5 \Pi_{MnCu} \times (-1)^{S+S_{Cu}+S_{Mn}} \begin{Bmatrix} S_{Mn}^* & S_{Cu} & S \\ S_{Cu} & S_{Mn} & 1 \end{Bmatrix} \langle \alpha S_{Mn} | S_{Mn} | \alpha^* S_{Mn}^* \rangle \langle S_{Cu} | S_{Cu} | S_{Cu} \rangle$$

The reduced matrix element for $Cu(II)$ ($S_{Cu} = 1/2$) is

$$\langle S_{Cu} | S_{Cu} | S_{Cu} \rangle = \sqrt{S_{Cu}(S_{Cu}+1)(2S_{Cu}+1)} = \sqrt{3/2}$$

The matrix elements for the $Mn(II)$ ions may be written as

$$\langle \alpha S_{Mn} | S_{Mn} | \alpha^* S_{Mn}^* \rangle = \langle f_0 | S_{Mn} | (1/\sqrt{2})(f_1 \pm f_2) \rangle$$

with

$$\langle f_0 | = \langle S_{Mn1} = 5/2, S_{Mn2} = 5/2, S_{Mn} |$$

$$|(f_1 \pm f_2)\rangle = |S_{Mn1} = 5/2, S_{Mn2} = 3/2, S_{Mn}^* \rangle \pm |S_{Mn1} = 3/2, S_{Mn2} = 5/2, S_{Mn}^* \rangle$$

The reduced matrix elements $\langle f_0 | S_{Mn} | f_i \rangle$ are calculated using the expression

(36) Weissbluth, M. *Atoms and molecules*; Academic Press: London, 1978.

$$\langle f_0 | S_{Mn} | f_1 \rangle = (-1)^{5/2+3/2+S_{Mn}+1} \sqrt{(2S_{Mn}+1)(2S_{Mn}^*+1)} \times \begin{Bmatrix} S_{Mn} & 1 & S_{Mn}^* \\ 3/2 & 5/2 & 5/2 \end{Bmatrix} \langle S_{Mn1} = 5/2 | S_{Mn} | S_{Mn1} = 3/2 \rangle$$

Finally, the $\langle S_{Mn1} = 5/2 | S_{Mn} | S_{Mn1} = 3/2 \rangle$ matrix elements are taken from ref 16. A similar expression may be obtained for $\langle f_0 | S_{Mn} | f_2 \rangle$.

Using the relations between the Π_{MnCu} coefficients results in

$$\langle S_{Mn1} | S_{Mn} | S_{Mn1} \rangle \langle S_{Cu} | S_{Cu} | S_{Cu} \rangle \Pi_{Mn1Cu} = -\langle S_{Mn2} | S_{Mn} | S_{Mn2} \rangle \langle S_{Cu} | S_{Cu} | S_{Cu} \rangle \Pi_{Mn2Cu}$$

hence

$$\langle f_0 | S_{Mn} | f_1 \rangle \langle S_{Cu} | S_{Cu} | S_{Cu} \rangle \Pi_{Mn1Cu} = (-1)^{S_{Mn}+1} A$$

$$\langle f_0 | S_{Mn} | f_2 \rangle \langle S_{Cu} | S_{Cu} | S_{Cu} \rangle \Pi_{Mn2Cu} = (-1)^{S_{Mn}+1} A$$

where the vectorial constant A is

$$\sqrt{3/2} \sqrt{(2S_{Mn}+1)(2S_{Mn}^*+1)} \begin{Bmatrix} S_{Mn} & 1 & S_{Mn}^* \\ 3/2 & 5/2 & 5/2 \end{Bmatrix} \times (3 \sum_{i=d_x^2-y^2, d_z^2} \Pi_{MnCu} - 2 \sum_{j=d_{xy}, d_{xz}, d_{yz}} \Pi_{MnCu})$$

The $\Delta S_{Mn} = 0$ subtransitions have nonzero transition moments when the function associated with the excited state contains $|f_1 + f_2\rangle$. On the other hand, the $\Delta S_{Mn} = \pm 1$ subtransitions have nonzero transition moments when the function associated with the excited state contains $|f_1 - f_2\rangle$.

Finally, the $P(S, S_{Mn}, S_{Mn}^*)$ effective transition moments associated with the 16 parity-allowed subtransitions are expressed as

$$P(S, S_{Mn}, S_{Mn}^*) = C \sqrt{(2S_{Mn}+1)(2S_{Mn}^*+1)} \times \begin{Bmatrix} S_{Mn}^* & 1/2 & S \\ 1/2 & S_{Mn} & 1 \end{Bmatrix} \begin{Bmatrix} S_{Mn} & 1 & S_{Mn}^* \\ 3/2 & 5/2 & 5/2 \end{Bmatrix}$$

where C is

$$\sqrt{3/2} (3 \sum_{i=d_x^2-y^2, d_z^2} \Pi_{MnCu} - 2 \sum_{j=d_{xy}, d_{xz}, d_{yz}} \Pi_{MnCu})$$